Efficient rectifier circuit operating at N78 and N79 sub-6 GHz 5G bands for microwave energy-harvesting and power transfer applications

Md. Ahsan Halimi[1,2] (iD), Taimoor Khan[1] (iD), Ahmed A. Kishk[3] (iD) and Yahia M.M. Antar[4] (iD)

[1]Department of Electronics and Communication Engineering, National Institute of Technology Silchar, Silchar, India ; [2]Department of Electronics and Communication Engineering, V R Siddhartha Engineering College, Vijayawada, India; [3]Department of Electrical and Computer Engineering, Concordia University, Montreal, Quebec, Canada and [4]Department of Electrical and Computer Engineering, Royal Military College of Canada, Kingston, ON, Canada

CAMBRIDGE UNIVERSITY PRESS

Abstract

The microwave energy-harvesting (MEH) and microwave power transfer (MPT) technologies have become the most emerging areas of research nowadays. The microwave rectifier circuit is the bottleneck of both the MEH and MPT systems. The efficiency of the system depends on the power conversion efficiency (PCE) of the rectifier. Due to the recent advancement of the fifth-generation communication system, it is desirable to propose an efficient rectifier operating at sub-6 GHz 5G bands. A dual-band rectifier circuit is designed and demonstrated for MEH/MPT purposes, specifically at sub-6 GHz 5G frequency bands. The dual-band matching is achieved by using a stepped impedance transmission line. The rectifier covers N78 (3.3–3.6 GHz) and N79 (4.8–5.0 GHz) bands. Peak PCE of 67.6% @ 3.5 GHz and 56.8% @ 4.9 GHz are achieved. For validation purpose, the rectifier is fabricated and characterized and measured results show good agreement with simulated results.

Introduction

With the invention of rectenna (rectifying antenna), microwave energy-harvesting (MEH) and microwave power transfer (MPT) technologies have received wide notice in the research and industry. Rectennas give MEH and MPT systems flexibility in terms of physical wiring, battery charging, and periodic replacement. Such systems have found applications in wireless charging of mobile phones or any electric/electronic equipment, radio-frequency (RF) identification (RFID) tags, Internet of Things, implantable/wearable biomedical devices, wireless sensors, and devices in the smart home [1–3]. Wi-Fi, GSM, LTE, and third/fourth/fifth generation (3G/4G/5G) are some wireless communication systems that radiate electromagnetic power in the environment. Radiation from these systems may serve as a source of electromagnetic energy that may harvest using an appropriate rectenna. Rectifying antenna A rectenna consists of an antenna, and rectifier, through a matching circuit. The rectifier is the crucial component of the rectenna for converting microwave energy into electrical direct current (DC). Therefore, several recent studies have been conducted to introduce efficient rectifier circuits [4–8]. The popular rectifier topologies are series diode [9], shunt diode [10], voltage doubler (VD) [11], and Greinacher full-wave rectifiers [12]. VD topology doubles the output voltage and improves the power handling capability for low power requirements [13]. The matching circuit is very essential for maximum power transfer from the antenna to the rectifier. To know the input impedance of the rectifier is necessary for proper matching network (MN) design. The operating frequency and input power level affect the input impedance of the rectifier. Hence, it is very difficult to find impedance matching at two or more frequencies simultaneously [14–16]. A dual-band rectifier (DBR) has the potential to utilize two bands simultaneously which can improve the output power levels. In recent years, many techniques have been adopted to design a DBR. In paper [17], a rectifier using an impedance matching network (IMN), having three lumped inductors and a radial stub, was designed to work at 0.915 and 2.45 GHz, simultaneously. A dual-band matching was realized using cascaded L-type and π-type networks to design a DBR circuit working at 0.915 and 2.45 GHz bands [18]. In paper [19], two-branch IMN was utilized to match within the 0.9 GHz UHF and 2.45 GHz ISM bands using a T-type MN. In paper [20], a DBR circuit consisting of a band-stop filter (BSF), a short-ended quarter-wave transmission line (QWTL) in series with a shunt diode, and a short-ended quarter-wave stub

Table 1. Sub-6 GHz fifth-generation bands

Band	Nation	Bandwidth
N78	Europe	3.4–3.8 GHz
N78	Korea	3.42–3.7 GHz
N78, N79	China	3.3–3.6 & 4.8–5 GHz
N78	India	3.3–3.6 GHz

was proposed. Here, BSF and QWTL were applied to block the second harmonic at 2.45 and 5.8 GHz, respectively. A short-ended quarter-wave stub was applied for impedance tuning at the first band. In papers [21, 22], dual-band IMN at 2.45 and 5.8 GHz has been designed by tuning the characteristic impedance (width) of a quarter-wave short-ended stub. A dual-band matching at 0.915 and 2.45 GHz was realized using a stepped impedance stub (SIS) [23]. The uniform width stub was cut out to form a SIS to find matching at two resonance bands to design a DBR. In paper [24], a DBR was designed using lumped component-based modified T-section IMN. The DBRs above targeted GSM 0.9 GHz, GSM 1.8 GHz, ISM 2.45 GHz, and ISM 5.8 GHz bands. However, the commercialization of fifth-generation (5G) wireless communication has gained attention to the design of a rectifier operating at sub-6 GHz 5G bands. Some of the DBRs are reported at one of the 5G bands. DBR was reported to operate at 2.45 GHz Wi-Fi and 3.5 GHz 5G using composite left/right-handed-based IMN [25], short-ended stub IMN [26], and two-branch IMN [27]. In [28–30], DBRs were proposed to work at 3.5 and 5.8 GHz bands. In paper [31], a rectifier has been designed using π-type dual-band IMN with a dual-band harmonic termination network (HTN). In paper [32], a DBR using two-branch IMN was utilized to work at 2.45 and 5 GHz. In paper [33], a three-stage Villard DBR was designed to operate at 2.4 and 5.2 GHz.

All of these rectifiers have relatively low efficiencies. Also, the DBR reported in papers [25–33] does not focus on dual 5G bands. In paper [34], a Greinacher full-wave rectifier circuit was developed to operate at dual 5G bands, and at 12 dBm input, it achieved 22.7% and 30.7% power conversion efficiency (PCE) at 3.5 and 5.0 GHz, respectively. In paper [35], a transparent and flexible dual-band 5G rectifier was reported, but the achieved PCE at 13 dBm was 54.67% and 7% at N78 and N79 bands, respectively, which is very poor, especially at the N79 band. Hence, it is desirable to develop an efficient and compact rectifier circuit to harvest RF energy of sub-6 GHz dual 5G bands. The 5G bands adopted in some nations are displayed in Table 1 [36] which is self-explanatory.

The short-ended stub [20–22], stepped impedance short-ended stub [23], composite right/left-handed structure [25], half-wavelength transmission line (TL) [30], π-type dual-band IMN with dual-band HTN [31], cross-branch dual-stub [34], and combination of open and short-ended stub [37] were utilized in some of the existing designs to achieve dual-band matching. The proposed design uses a novel stepped impedance TL technique to satisfy the matching at two sub-6 GHz fifth-generation (5G) bands. Hence, the novelty of the proposed dual-band 5G rectifier is in terms of (a) dual 5G bands with better performance compared to existing ones and (b) a novel dual-band matching technique using a stepped impedance TL.

This paper demonstrates an efficient DBR circuit covering 3.3–3.7 GHz (N 78 band adopted by India, China, Europe, and Korea) and 4.8–5.0 GHz bands (N 79 band adopted by China).

The power/frequency-weighted efficiency (PFE) has been derived to compare the overall circuit performance including frequency of operation and operating power level. The proposed work exhibits the highest PFE. The rest of this paper is arranged as follows. The "Dual-band rectifier" discusses the geometric description and simulated results of the proposed DBR circuit. The "Fabrication, measurement, and comparison" section discusses the fabrication and characterization of the rectifier. Finally, the work is concluded in the "Conclusion" section.

Dual-band rectifier

The design of a DBR is auspicious to operate at sub-6 GHz 5G bands. For this, a dual-band MN is needed. It is very challenging to design an MN satisfying two different operating frequencies because of the diode's nonlinear nature. One of the methods is to combine two rectifiers operating at two different operating frequencies. The second method is to utilize a single dual-band MN. The proposed design uses a novel stepped impedance TL to satisfy the matching at two sub-6 GHz fifth-generation (5G) bands.

Geometrical description

Figure 1(a) and (b) displays the schematic and layout view of the proposed DBR circuit. The SOT-23 package of HSMS-2862 (VD topology) is used in the proposed rectifier. The substrate used in this design is RO4003 (dielectric constant = 3.55, loss tangent = 0.0027, and thickness = 1.524 mm). The MN is based on stepped impedance TL segments of different lengths. For simplification, the principle of dual-band impedance transformation is analyzed using lossless TL theory [38]. The impedance Z_a across the TL, TL_1 can be calculated using (1):

$$Z_{a@f_i} = Z_{0TL1} \frac{Z_{L@fi} + jZ_{0TL1} \tan \beta_{fi} L_{TL1}}{Z_{0TL1} + jZ_{L@fi} \tan \beta_{fi} L_{TL1}} \quad (1)$$

Here, "i" denotes 1 and 2 of the DBR's first and second bands, f_1 and f_2, respectively. The impedance Z_b, Z_c, and Z_{in} across the TL_2, TL_3, and TL_4, respectively, can be calculated using (2), (3), and (4), respectively:

$$Z_{b@f_i} = Z_{0TL2} \frac{Z_{a@fi} + jZ_{0TL2} \tan \beta_{fi} L_{TL2}}{Z_{0TL2} + jZ_{a@fi} \tan \beta_{fi} L_{TL2}} \quad (2)$$

$$Z_{c@f_i} = Z_{0TL3} \frac{Z_{b@fi} + jZ_{0TL3} \tan \beta_{fi} L_{TL3}}{Z_{0TL3} + jZ_{b@fi} \tan \beta_{fi} L_{TL3}} \quad (3)$$

$$Z_{in@f_i} = Z_{0TL4} \frac{Z_{c@fi} + jZ_{0TL4} \tan \beta_{fi} L_{TL4}}{Z_{0TL4} + jZ_{c@fi} \tan \beta_{fi} L_{TL4}} \quad (4)$$

For matching at two frequencies, f_1 and f_2, the real and imaginary parts of the input impedance Z_{in} should follow the criteria of (5) and (6).

$$\text{Re}\left(Z_{in@f_1}\right) \approx \text{Re}\left(Z_{in@f_2}\right) \approx 50 \, \Omega \quad (5)$$

$$\text{Im}\left(Z_{in@f_1}\right) \approx \text{Im}\left(Z_{in@f_2}\right) \approx 0 \, \Omega \quad (6)$$
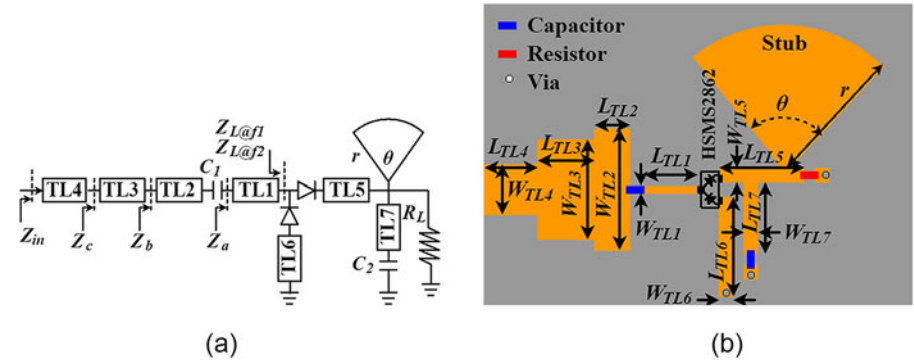
Figure 1. Image of dual-band rectifier: (a) Schematic view and (b) Layout view.
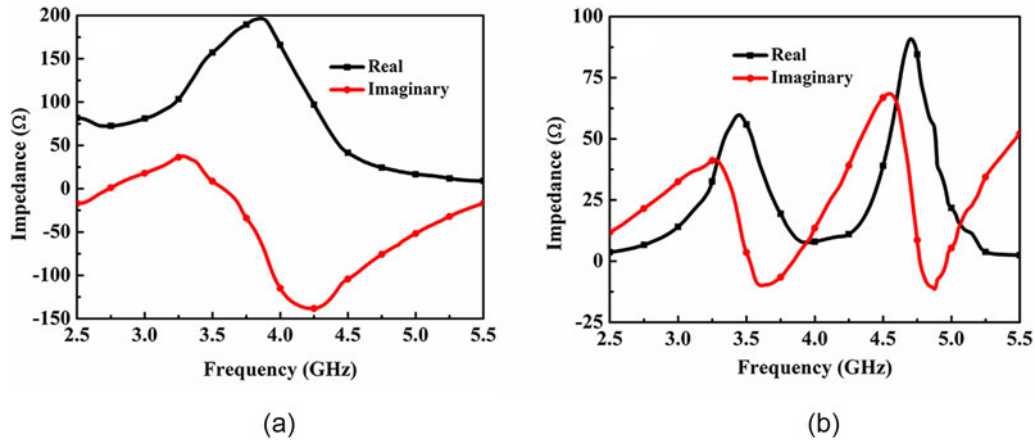

Figure 2. Input impedance of rectifier (a) without MN (Z_L) and (b) with an MN (Z_{in}).

The matching at two frequency bands is achieved by tuning the TL parameters. The 3.5 and 4.9 GHz dual sub-6 GHz 5G bands are selected as f_1 and f_2, respectively.

Figure 2(a) shows the input impedance of the rectifier circuit without using the MN are $Z_{L@f1} = 157 + j8\ \Omega$ and $Z_{L@f2} = 20 - j61\ \Omega$. After introducing a MN using the source pulling technique, Fig. 2(b) shows the input impedance of the rectifier becomes, $Z_{in@3.53\ GHz} = 52 - j1\ \Omega$ and $Z_{in@4.89\ GHz} = 45 - j9\ \Omega$ which satisfies (5) and (6). The optimal dimensions of the TLs (in mm) are; $L_{TL1} = 4.5$, $L_{TL2} = 4.2$, $L_{TL3} = 5$, $L_{TL4} = 3.8$, $L_{TL5} = 6$, $L_{TL6} = 6.4$, $L_{TL7} = 3.8$, $W_{TL1} = 1$, $W_{TL2} = 8.6$, $W_{TL3} = 7$, $W_{TL4} = 3.6$, $W_{TL5} = W_{TL6} = 1$, $W_{TL7} = 1.1$, radius of fan-shaped stub $r = 9$ and angle $\theta = 60°$.

Simulated results and discussion

The rectifier circuit is simulated using Keysight advanced design system. At different values of input power levels, the simulated S_{11} vs. frequency is depicted in Fig. 3(a). The result shows that the circuit is well-matched at both 3.5 GHz and 4.9 GHz 5G bands. The PCE in the desired band is simulated for different load values and input power. The PCE vs. P_{in} at 3.5 and 4.9 GHz is displayed in Fig. 3(b). The maximum PCE is 70.6% @6 dBm and 62.9% @ 5 dBm at 3.5 and 4.9 GHz, respectively, for a 3 kΩ load. The simulated PCE is greater than 50% for the input power range from −2.5 to 12.4 and −0.8 to 8.3 dBm for 3.5 and 4.9 GHz, respectively. PCE vs. load is depicted in Fig. 3(c) at 0, 3, and 6 dBm input power levels at both frequencies. With the increase of load value, PCE starts increasing and reached its maximum value, and then

starts decreasing. Hence, a 3-kΩ resistor is selected as the optimum load to better perform at an input power level between −10 and 10 dBm.

Figure 3(d) shows the PCE vs. frequency graph. The maximum simulated PCE at two different bands is 72.8% and 67.2% at 3.55 and 4.94 GHz at 6 dBm. PCE is higher than 60%, from 3.35 to 3.83 and 4.83 to 5.09 GHz. At a 3 dBm power level, the PCE is higher than 55% from 3.3 to 3.74 and 4.8 to 5.0 GHz. PCE is 61.4% and 53.5% at 3.45 and 4.8 GHz, respectively, at 0 dBm. The V_{out} vs. frequency at −3, 0, 3, and 6 dBm input power levels are displayed in Fig. 3(e). At 3 dBm, the V_{out} is greater than 1.5 V for both bands from 3.1 to 3.84 and 4.6 to 5.07 GHz. Also, the V_{out} is more than 2.5 V from 3.28 to 3.86 and 4.76 to 5.13 GHz.

Fabrication, measurement, and comparison

For the endorsement of the proposed 5G rectifier, an experimental setup is depicted in Fig. 4(a). Figure 4(b) describes the fabricated prototype of the proposed DBR. The RF signal generator was used for input power feeding to the rectifier circuit, and a digital meter was used for output voltage measurement. The output DC voltage was noted, and the PCE was calculated using (7).

$$\mathrm{PCE} = \frac{V_{out}^2}{R_L * P_{in}} \times 100\% \qquad (7)$$

Figure 5(a) shows the measured S11 (bottom left negative y-axis), Vout (right y-axis), and PCE (top left positive y-axis) vs.
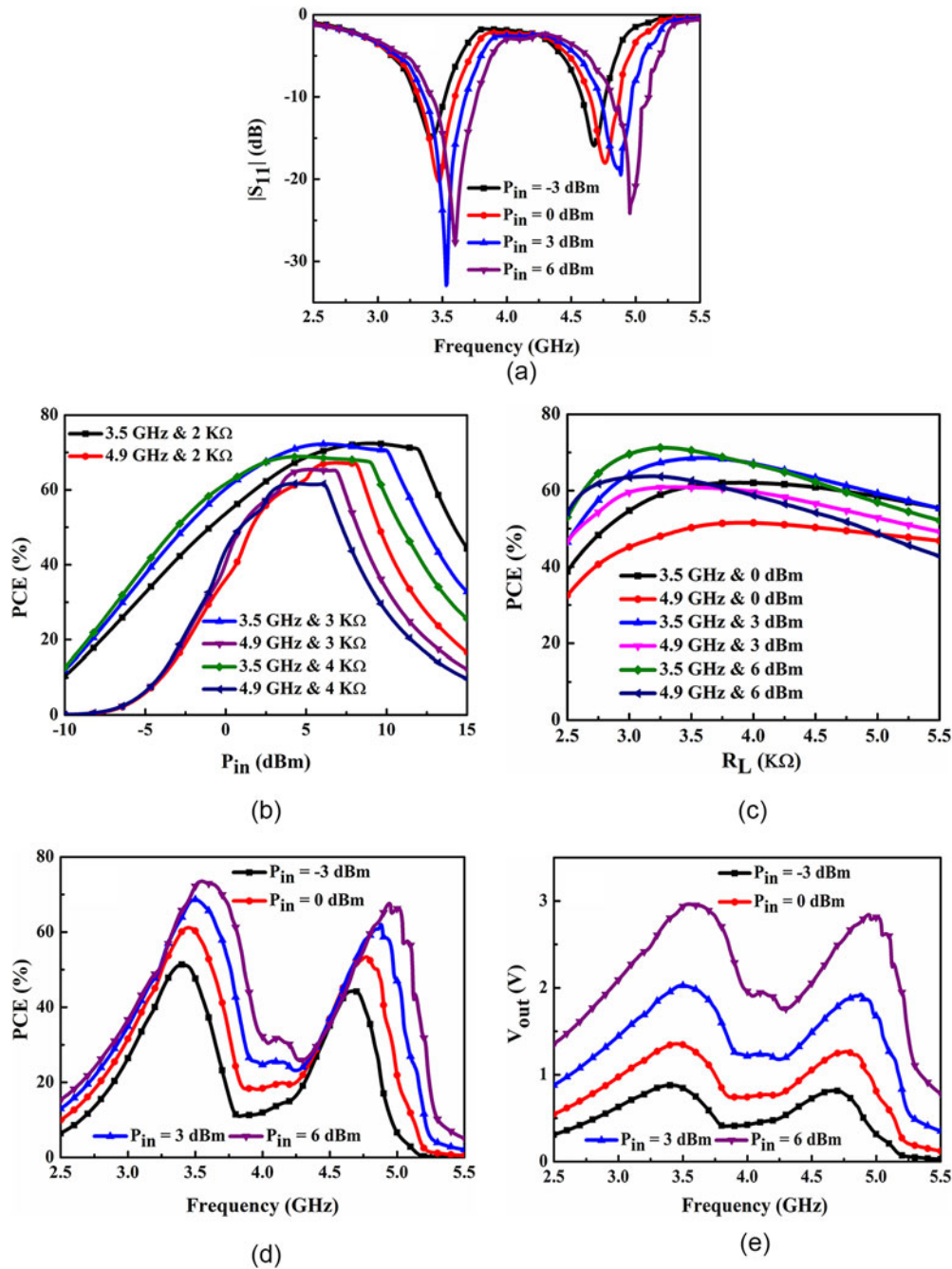
Figure 3. Simulated performance: (a) S_{11} vs. frequency, (b) PCE vs. input power (P_{in}), (c) PCE vs. load (R_L). (d) PCE vs. frequency, and (e) V_{out} vs. frequency.

frequency, respectively at 6 dBm input power. Load resistance of 3 kΩ and input power of 0 dBm are applied to the rectifier. The measured value of $|S_{11}|$ is −28.9 and −16.2 dB at 3.7 and 5.0 GHz respectively. The maximum recorded DC output voltage is 2.96 and 2.77 V at 3.7 and 5.05 GHz, respectively. The PCE is more than 50% for 3.25–3.96 and 4.81–5.15 GHz bands. Figure 5(b) and (c) show the V_{out} and PCE vs. P_{in}, respectively. The measured DC output voltages recorded are 1.32 V @ 0 dBm and 2.53 V @ 5 dBm at 3.5 GHz, respectively. At 4.9 GHz, the output voltages are 1.26 V @ 0 dBm and 2.31 V @ 5 dBm. At 3.5 GHz, the measured PCE is 58.1% @ 0 dBm, 67.3% @ 5 dBm, and the maximum PCE reached 67.6% @ 6 dBm input power.

The measured value of PCE at 4.9 GHz is 52.8% at 0 dBm, 56.3% at 5 dBm, and the peak PCE reached 56.8% at 3.5 dBm input power. Measured results show good agreement with the simulated ones. The little difference between simulated and measured performance may be due to diode model inaccuracies and fabrication tolerance.

Table 2 describes the comparison of the 5G DBR performance with some existing works. The rectifier achieved 58.1% and 52.8% PCE at 0 dBm for operating frequencies 3.5 and 4.9 GHz, respectively. The PCE at 0 dBm of existing rectifiers presented in papers [24, 26, 27, 39] looks better because of the lower operating frequency (band). Because of the skin effect and parasitic effects,
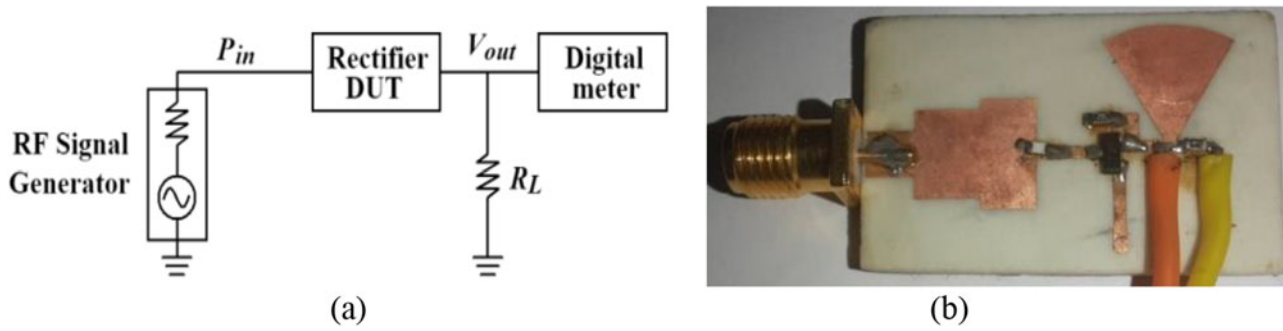
Figure 4. (a) Measurement setup, (b) rectifier prototype.

(a)

(b)

(c)
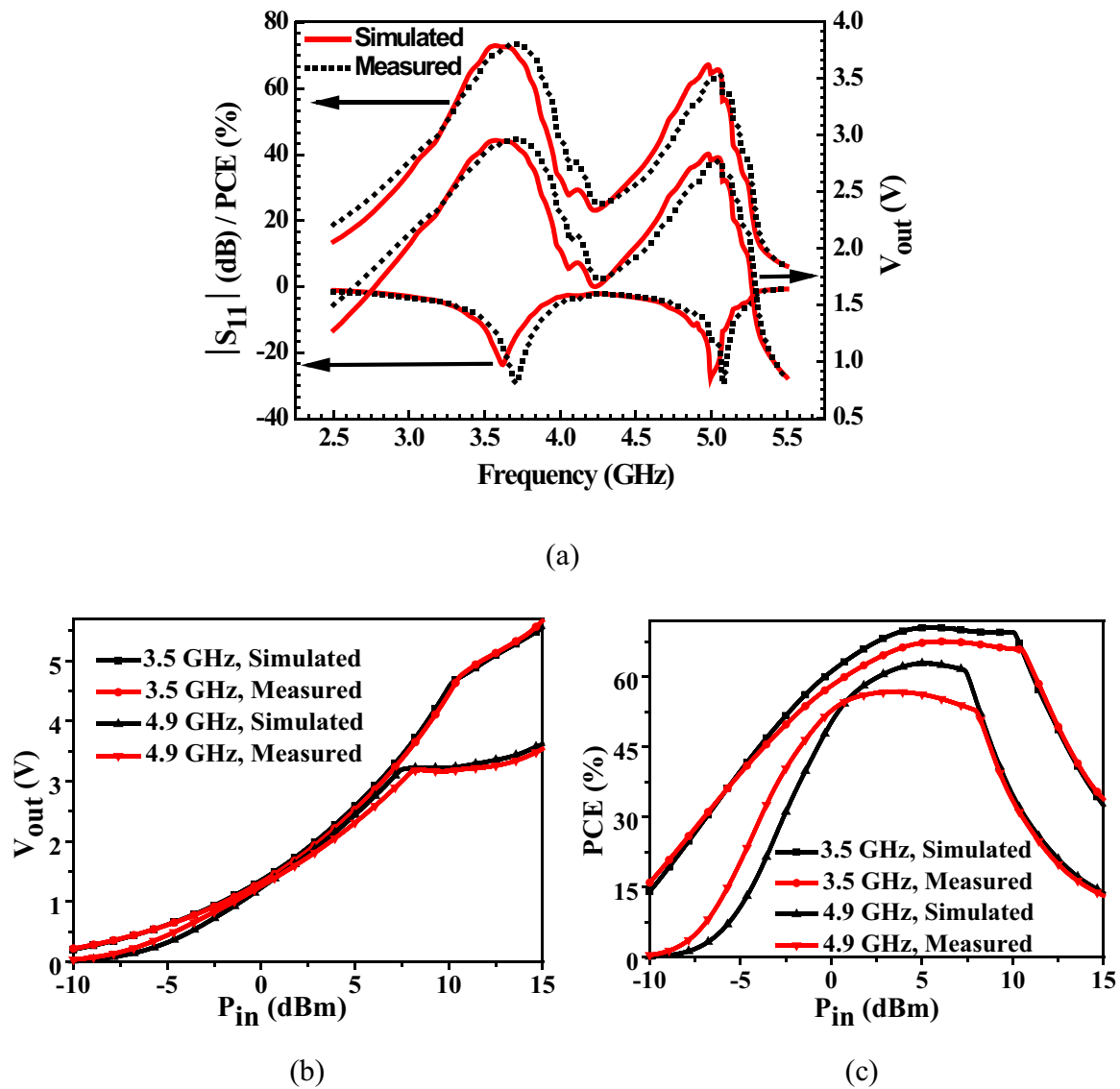
Figure 5. Measured results of (a) S_{11}, PCE, V_{out} vs. frequency, (b) V_{out}, vs. P_{in}, (c) PCE vs. P_{in}.

the loss increases at a high operating frequency. Therefore, to compare DBRs operating at different bands, a frequency-weighted efficiency (FE) can be calculated using (8) [39]. The PCE presented in papers [31, 39] looks better because of the higher input power level. As the PCE of the rectifier circuit is also influenced by input

power level, a new PFE is presented in (9) to compare the overall circuit performance.

$$FE = \sum_{i=1}^{n} [\eta_i f_i^{0.25}] \qquad (8)$$

Table 2. Comparison with existing works

Reference/Year	Frequency (GHz)	Diode and topology	P_{in}(dBm)	PCE(%)	FE	PFE
[24]/2023	1.4/2.45	SMS7630 in VD	0	65/57	141.65	141.65
[39]/2023	1.81/2.35	HSMS2860 in Class F^{-1}	13	76.3/76.2	182.85	135.51
[36]/2023	3.5	HSMS2862 in VD	0	59	80.7	80.7
[25]/2020	2.5/3.6	SMS7630 in VD	2	59/41	130.66	124.82
[26]/2018	2.4/3.5	SMS7630 in Series	0	59/56	150.03	150.03
[27]/2019	2.45/3.5	HSMS 2852 in Greinacher	0	60/53	147.56	147.56
[28]/2020	3.5/5.8	SMS7630 in series	0	44/29	105.19	105.19
[29]/2021	3.5/5.8	HSMS2860 in Series	0	45.6/33	113.58	113.58
[30]/2022	3.5/5.8	HSMS2860 in Series	0	51.8/39.7	131.37	131.37
[37]/2022	2.6/3.5	SMS7630 in Series	−5	53/53	139.79	156.86
[31]/2023	2.32/3.48	SMS7621 in Class F^{-1}	5	64.5/64.2	167.29	149.11
[32]/2019	2.45/5.0	HSMS286B in VD	0	30.6/36.7	93.01	93.01
[33]/2023	2.4/5.2	SMS7630 in 3-stage Villard	0	69.1/35.1	139.01	139.01
[34]/2023	3.5/5.0	HSMS286C in Greinacher	12	22.7/30.7	76.96	58.38
[35]/2022	3.5/5.0	HSMS286C in VD	13	54.7/7	85.26	63.19
Proposed	**3.5/4.9**	**HSMS2860 in VD**	**0**	**58.1/52.8**	**158.02**	**158.02**
			5	**67.3/56.3**	**175.81**	**155.98**

FE: frequency-weighted efficiency FE. PFE: power/frequency-weighted efficiency.

$$\text{PFE} = \frac{1}{P_{in}^{0.1}} \times \text{FE} \qquad (9)$$

where n is the number of bands, f_i is the ith frequency band, η_i is the PCE at ith frequency band, and P_{in} is input power level in mW.

The power factor of input power in the denominator of (9) is decided based on the proposed circuit FOM at two different power levels (0 and 5 dBm). The circuit performance is found approximately equal using this overall PFE (i.e., approximately 158 and 156 at 0 and 5 dBm, respectively).

Conclusion

A rectifier to operate at dual sub-6 GHz 5G band has been designed. An HSMS2862 in the SOT-23 package (VD configuration) has been employed for RF to DC conversion. A stepped impedance TL-based MN has been utilized to transform the rectifier input impedance close to 50 Ω at both operating bands. The rectifier efficiently covers the 3.5 GHz (N78 band) and 4.9 GHz (N79 band) bands of fifth-generation wireless communication. A maximum PCE of 67.6% at 3.5 GHz and 56.8% at 4.9 GHz has been achieved. These characteristics make this rectifier a good candidate for MEH and MPT systems. Future work includes improving the sensitivity of the rectifier and a dual-band 5G antenna design to implement a rectenna circuit.

Competing interests. The authors report no conflict of interest.

References

1. **Surender D, Halimi MA, Khan T, Talukdar FA and Rengarajan SR** (2022) 5G /Millimeter-wave rectenna systems for radio-frequency energy harvesting/wireless power transmission applications: An overview. *IEEE Antennas and Propagation Magazine.* **65**(3), 57–76.
2. **Rahmani H, Shetty D, Wagih M, Ghasempour Y, Palazzi V, Carvalho NB, Correia R, Costanzo A, Vital D, Alimenti F and Kettle J** (2023) Next-generation IoT devices: Sustainable eco-friendly manufacturing, energy harvesting, and wireless connectivity. *IEEE Journal of Microwaves* **3**(1), 237–255.
3. **Hussein SH and Mohammed KK** (2023) A miniaturized advanced rectenna integrated circuit for implantable applications. *AEU - International Journal of Electronics and Communications* **161**, 154544.
4. **Halimi MA, Khan T, Nasimuddin AAK and Antar YMM** (2023) Rectifier circuits for RF energy harvesting and wireless power transfer applications: A comprehensive review based on operating conditions. *IEEE Microwave Magazine* **24**(1), 46–61.
5. **Halimi MA, Khan T, Palandoken M, Kishk AA and Antar YMM** (2023) Rectifier design challenges for wireless energy harvesting/wireless power transfer systems: Broadening bandwidth and extending input power range. *IEEE Microwave Magazine* **24**(6), 54–67.
6. **Collado A, Daskalakis SN, Niotaki K, Martinez R, Bolos F and Georgiadis A** (2017) Rectifier design challenges for RF wireless power transfer and energy harvesting systems. *Radioengineering* **26**(2), 411–417.
7. **Halimi MA, Khan T, Surender D, Nasimuddin N and Rengarajan SR** (2023) Dielectric resonator antennas for RF energy-harvesting/wireless power transmission applications: A state-of-the-art review. *IEEE Antennas and Propagation Magazine*, Early access.
8. **Surender D, Halimi MA, Khan T, Talukdar FA, Kanaujia BK, Rambabu K and Kishk AA** (2023) Analysis of facet-loaded rectangular DR-rectenna designs for multisource RF energy-harvesting applications. *IEEE Transactions on Antennas and Propagation* **71**(2), 1273–1284.

9. **Halimi MA, Surender D, Khan T, Kishk AA and Rengarajan SR** (2022) A multistepped transmission line matching strategy based triple-band rectifier for RFEH/WPT applications. *IEEE Microwave and Wireless Components Letters* **32**(8), 1007–1010.

10. **Meher PR, Mishra SK and Halimi MA** (2023) A low-profile compact broadband CP DRA for RF energy harvesting applications. *IETE Journal of Research*, 1–9.

11. **Halimi MA, Khan T, Kishk AA and Rengarajan SR** (2022) Design of a frequency selectable rectifier using tuned matching circuit for RFEH applications. *IETE Journal of Research*, 1–9.

12. **Gozel MA, Kahriman M and Kasar O** (2018) Design of an efficiency-enhanced Greinacher rectifier operating in the GSM 1800 band by using rat-race coupler for RF energy harvesting applications. *International Journal of RF and Microwave Computer Aided Engineering* **29**(1), 1–8.

13. **Halimi MA, Surender D and Khan T** (2021) Design of a 2.45 GHz operated rectifier with 81.5% PCE at 13 dBm input power for RFEH/WPT applications. In *2021 IEEE Indian Conference on Antennas and Propagation (InCAP)*, 981–983.

14. **Shieh S and Kamarei M** (2018) Transient input impedance modeling of rectifiers for RF energy harvesting applications. *IEEE Transactions on Circuits and Systems II: Express Briefs* **65**(3), 311–315.

15. **García-Moreno S, Gurrola-Navarro MA, Bonilla-Barragán CA and Mejía I** (2020) Design method for RF energy harvesting rectifiers. *IEEE Transactions on Circuits and Systems II: Express Briefs* **67**(11), 2727–2731.

16. **Trevisoli R, D. Paz HP, D. Silva VS, Doria RT, Casella IRS and Capovilla CE** (2022) Modeling Schottky diode rectifiers considering the reverse conduction for RF wireless power transfer. *IEEE Transactions on Circuits and Systems II: Express Briefs* **69**(3), 1732–1736.

17. **Niotaki K, Kim S, Jeong S, Collado A, Georgiadis A and Tentzeris MM** (2013) A compact dual-band rectenna using slot-loaded dual band folded dipole antenna. *IEEE Antennas and Wireless Propagation Letters* **12**, 1634–1637.

18. **Liu J, Zhang XY and Yang CL** (2017) Analysis and design of dual-band rectifier using novel matching network. *IEEE Transactions on Circuits and Systems II: Express Briefs* **65**(4), 431–435.

19. **Quddious A, Zahid S, Tahir FA, Antoniades MA, Vryonides P and Nikolaou S** (2020) Dual-band compact rectenna for UHF and ISM wireless power transfer systems. *IEEE Transactions on Antennas and Propagation* **69**(4), 2392–2397.

20. **Jiang W, Liu C, Huang K, Huang K and Huang K** (2013) A novel dual-frequency microwave rectifier at 2.45 and 5.8 GHz with harmonic recycling. *Journal of Electromagnetic Waves and Applications* **27**(6), 707–715.

21. **Wang D and Negra R** (2013) Design of a dual-band rectifier for wireless power transmission. In *2013 IEEE Wireless Power Transfer (WPT)*, 127–130.

22. **Huang XB, Wang JJ, Wu XY and Liu MX** (2015) A dual-band rectifier for low-power Wireless Power Transmission system. In *2015 Asia-Pacific Microwave Conference (APMC)*, vol. 2, 1–3.

23. **Li S, Cheng F, Gu C, Yu S and Huang K** (2021) Efficient dual-band rectifier using stepped impedance stub matching network for wireless energy harvesting. In *IEEE Microwave and Wireless Components Letters*.

24. **Dubey R, Srivastava SK, Singh A and Meshram MK** Compact and efficient dual-band rectifier using modified T-Section matching network. In *IEEE Microwave and Wireless Technology Letters*.

25. **Chandrasekaran KT, Agarwal K, Alphones A, Mittra R and Karim MF** (2020) Compact dual-band metamaterial-based high-efficiency rectenna: An application for ambient electromagnetic energy harvesting. *IEEE Antennas and Propagation Magazine* **62**(3), 18–29.

26. **Eltresy N, Eisheakh D, Abdallah E and Elhenawy H** (2018) RF energy harvesting using efficiency dual band rectifier. In *2018 Asia-Pacific Microwave Conference (APMC)*, 1453–1455.

27. **Wang M, Fan Y, Yang L, Li Y, Feng J and Shi Y** (2019) Compact dual-band rectenna for RF energy harvest based on a tree-like antenna. *IET Microwaves, Antennas & Propagation* **13**(9), 1350–1357.

28. **Derbal MC and Nedil M** (2020) A high gain dual band rectenna for RF energy harvesting applications. *Progress in Electromagnetics Research Letters* **90**, 29–36.

29. **Surender D, Halimi MA, Khan T, Talukdar FA and Antar YMM** (2022) Circularly polarized DR-rectenna for 5G and Wi-Fi bands RF energy harvesting in smart city applications. *IETE Technical Review* **39**(4), 880–893.

30. **Halimi MA, Khan T, Koul SK and Rengarajan SR** (2023) A dual-band rectifier using half-wave transmission line matching for 5G and Wi-Fi bands RFEH/MPT applications. In *IEEE Microwave and Wireless Technology Letters*, Vol. **33**(1), 74–77.

31. **Bui GT, Nguyen DA and Seo C** (2023) A novel design of dual-band inverse Class-F shunt-diode rectifier for energy harvesting. In *IEEE Transactions on Circuits and Systems II: Express Briefs*, Vol. **70**(7), 2345–2349.

32. **Noor FSM, Zakaria Z, Lago H and Said MAM** (2019) Dual-band aperture-coupled rectenna for radio frequency energy harvesting. *International Journal of RF and Microwave Computer-Aided Engineering* **29**(1), 1–9.

33. **Patil DD, Subramanian KS, Pradhan NC, Varadharaj EK, Senthilkumaran K and Murugesan M** (2023) 3D-printed dual-band energy harvester for WSNs in green IoT applications. *AEU - International Journal of Electronics and Communications* **164**, 154641.

34. **Bougas ID, Papadopoulou MS, Boursianis AD, Nikolaidis S and Goudos SK** (2023) Dual-band rectifier circuit design for IoT communication in 5G systems. *Technologies* **11**(2), 34.

35. **Yu BY, Wang ZH, Ju L, Zhang C, Liu ZG, Tao L and Lu WB** (2022) Flexible and wearable hybrid RF and solar energy harvesting system. *IEEE Transactions on Antennas and Propagation* **70**(3), 2223–2233.

36. **Halimi MA, Shome PP, Khan T and Rengarajan SR** (2023) Efficient single and broadband microwave rectifiers for RFEH/WPT enabled low power 5G sub-6 GHz device. *AEU - International Journal of Electronics and Communications* **165**, 1–8.

37. **Guo L, Li X, Sun W, Zhao Y and Wu K** (2022) Designing and modeling of a dual-band rectenna with compact dielectric resonator antenna. *IEEE Antennas and Wireless Propagation Letters* **21**(5), 1046–1050.

38. **Costantine J, Eid A, Abdallah M, Tawk Y and Ramadan AH** (2017) A load independent tapered RF harvester. *IEEE Microwave and Wireless Components Letters* **27**(10), 933–935.

39. **Nguyen DA, Bui GT, Nam H and Seo C** (2023) Design of dual-band inverse Class-F rectifier for wireless power transfer and energy harvesting. *IEEE Microwave and Wireless Technology Letters* **33**(3), 355–358.

Md. Ahsan Halimi received his B.Tech. and M.Tech. degrees in the stream of Electronics and Communication Engineering from Ajmer Institute of Technology, Ajmer, India, and Pondicherry University, Pondicherry, India, respectively. He is working as a PhD scholar at National Institute of Technology Silchar, India. Currently, he is an assistant professor with the Department of Electronics and Communication Engineering, V R Siddhartha Engineering College, Vijayawada, India. His research interest includes RF energy harvesting, microwave rectifiers, UWB antennas, reconfigurable antennas. Email: ahsanhalimi@gmail.com.

Taimoor Khan received his Ph.D. degree in Electronics and Communication Engineering from National Institute of Technology Patna, India. Presently he is an Assistant Professor in the Department of Electronics and Communication Engineering at the National Institute of Technology Silchar, Assam, since 2014. Before joining NIT Silchar, he served different organizations for around 15 years in different capacities like lab instructor, lecturer, assistant professor, and associate professor, respectively. His active research interest includes printed microwave circuits, electromagnetic bandgap structures, ultrawideband antennas, dielectric resonator antennas, ambient microwave energy harvesting, and artificial intelligence paradigms in electromagnetics. Corresponding author email: ktaimoor@ieee.org.

82

Halimi et al.

Ahmed A. Kishk received his Ph.D. degree from University of Manitoba, Winnipeg, Canada, in 1986. From 1977 to 1981, he was a research assistant and an instructor at the Faculty of Engineering, Cairo University. From 1981 to 1985, he was a research assistant at the Department of Electrical Engineering, University of Manitoba. From December 1985 to August 1986, he was a research associate fellow in the same department. In 1986, he joined the Department of Electrical Engineering, University of Mississippi, as an assistant professor. He was on sabbatical leave at the Chalmers University of Technology, Sweden, during the 1994–1995 and 2009–2010 academic years. He was a professor at the University of Mississippi (1995–2011). He was the director of the Center for Applied Electromagnetic System Research (CAESR) during the period 2010–2011. Currently, he is a professor at Concordia University, Montréal, Québec, Canada (since 2011) as Tier 1 Canada Research Chair in Advanced Antenna Systems. Email: kishk@encs.concordia.ca.

Yahia M. M. Antar joined the Division of Electrical Engineering, National Research Council of Canada. In 1987, he joined the Department of Electrical and Computer Engineering, Royal Military College of Canada, Canada, where he has been a professor since 1990. He was appointed as a member of the Canadian Defence Advisory Board of the Canadian Department of National Defence in 2011. He is a fellow of the Engineering Institute of Canada, the Electromagnetic Academy, and the International Union of Radio Science. He served as the Chair for Commission B from 1993 to 1999 and for CNC, URSI from 1999 to 2008, and has a cross-appointment at Queen's University, Kingston. In 2002, he was awarded a Tier 1 Canada Research Chair in electromagnetic engineering, which has been renewed in 2016. He serves as an associate editor for many IEEE and IET journals and as an IEEE-APS Distinguished Lecturer. He was elected by the URSI to the Board as the Vice President in 2008 and 2014 and by the IEEE AP AdCom in 2009. Presently, he is serving as President, IEEE APS (Region 7–10) for the year 2021. Email: antar-y@rmc.ca.

Downloaded from https://www.cambridge.org/core. Berklee College Of Music, on 11 Feb 2025 at 12:24:11, subject to the Cambridge Core terms of use, available at https://www.cambridge.org/core/terms.
https://doi.org/10.1017/S1759078723001162